

# Evaluation of Radiation-induced Luminescence Characteristics of Au Particles in CsCl Translucent Ceramic

Daiki Shiratori,<sup>1\*</sup> Hiromi Kimura,<sup>2</sup> Yutaka Fukuchi,<sup>1</sup> and Takayuki Yanagida<sup>3</sup>

<sup>1</sup>Department of Electrical Engineering, Tokyo University of Science,  
6-3-1 Nijjuku, Katsushika-ku, Tokyo 125-8585, Japan

<sup>2</sup>National Metrology Institute of Japan, National Institute of Advanced Industrial Science and Technology,  
1-1-1 Umezono, Tsukuba, Ibaraki 305-8568, Japan

<sup>3</sup>Division of Materials Science, Nara Institute of Science and Technology,  
8916-5 Takayama, Ikoma, Nara 630-0192, Japan

(Received October 30, 2023; accepted January 17, 2024)

**Keywords:** Au particle, radiation-induced luminescence, dosimeter, photoluminescence, translucent ceramic

In this study, the luminescence properties of Au-doped CsCl (ACC) translucent ceramics after irradiation were investigated with the aim of developing new radiation detection materials using Au nanoparticles. The prepared ACC translucent ceramics showed two main emissions (520 nm) upon UV-ray (~340 nm) irradiation, and the luminescence intensity after X-ray irradiation was found to change with time. We concluded that this luminescence behavior may be attributed to (i) the generation of luminescent Au nanoclusters (AuNCs) by X-ray irradiation or (ii) the excitation of AuNCs due to F-centers generated by X-ray irradiation, but a detailed study is needed to elucidate the mechanism. Moreover, as a result of investigating the variation in luminescence intensity with X-ray dose, it was found that there is a monotonically increasing dose range of luminescence intensity in the NIR region. This suggests that ACC functions as an X-ray detector in a specific dose region.

## 1. Introduction

One of the important applications using phosphors is radiation detection, such as that for personal dose monitoring<sup>(1–3)</sup> and in the fields of nuclear medicine,<sup>(4,5)</sup> security,<sup>(6,7)</sup> environmental dose monitoring,<sup>(8)</sup> oil logging,<sup>(9)</sup> and high-energy astronomy.<sup>(10)</sup> In these applications, radiation is measured by utilizing the regular change in the luminescence intensity of the phosphor relation to the energy of the irradiated ionizing radiation.<sup>(11–14)</sup> Passive detectors, such as personal dosimeters, accumulate radiation energy once as carriers and read it out later as photoluminescence (PL). There are two types of dosimeter classified by different ways (energies) to stimulate carriers; the thermally stimulated luminescence dosimeter uses thermal stimulation,<sup>(15–23)</sup> and the optically stimulated luminescence (OSL) dosimeter utilizes light stimulation.<sup>(24–29)</sup> In addition, some dosimeters use a phenomenon called radio-

---

\*Corresponding author: e-mail: [shiratori@rs.tus.ac.jp](mailto:shiratori@rs.tus.ac.jp)  
<https://doi.org/10.18494/SAM4764>

photoluminescence (RPL),<sup>(30–36)</sup> in which new luminescent centers corresponding to irradiation doses are generated, and RPL can be easily measured by a PL technique. In recent years, RPL materials have been expected to be used for imaging applications,<sup>(37–39)</sup> but only a few heavy-element RPL materials are suitable for radiation imaging such as X- or  $\gamma$ -ray imaging.

We propose a new heavy-element material doped with Au for radiation imaging. Au is a promising luminescent center for dosimeters because of its high atomic number and high probability of interacting with X- and  $\gamma$ -rays. In addition, nanoscale Au has some very interesting optical properties,<sup>(40)</sup> such as the surface plasmon effect (SPE) of Au nanoparticles (AuNPs).<sup>(41–43)</sup> In particular, the luminescence properties of Au nanoclusters (AuNCs) are some of the most remarkable. The AuNCs are Au particles with sizes smaller than those of AuNPs (approximately 0.3–20 nm), and the luminescence properties depend on different structural parameters such as particle size, surface ligands, and valence state as well as the AuNPs.<sup>(44)</sup> Namely, when the aggregation state of Au particles is changed by radiation, the optical properties of the Au particles are thereby changed; therefore, the changes can be utilized for radiation detection.

In this study, we focused on CsCl in the form of a translucent ceramic as a host material. The physical properties of CsCl itself have been investigated in depth previously,<sup>(45–48)</sup> and CsCl translucent ceramics have been shown to have excellent properties as dosimeter materials.<sup>(49)</sup> Moreover, in Au-doped chloride glasses, the luminescence due to Au particles has been observed, and the luminescence intensity has been found to vary with irradiation dose.<sup>(50)</sup> Therefore, CsCl was selected because it is suitable both as a radiation detection material and as a host material to which Au is doped.

## 2. Experimental Methods

### 2.1 Synthesis of ACC ceramic specimen

Au-doped CsCl (ACC) translucent ceramics with different concentrations of Au (0.03 and 1.0%) were synthesized by spark plasma sintering (SPS). Raw powders of CsCl (>99.999%, Mitsuwa Chemical Co., Ltd.) and AuCl (>99.99%, Strem Chemicals, Inc.) were homogeneously mixed at a molar ratio of 1: $x$  ( $x = 0.0003$  and  $0.01$ ) using an agate mortar and pestle. Then, the mixture (total mass: 0.5 g) was loaded in a cylindrical graphite die (inner diameter: 10.4 mm), in which the mixture was held between two graphite punches inserted in the cylinder. Then, the graphite die with the punches and mixture was placed in the chamber of the SPS furnace (Sinter Land, LABOX-110) to sinter the powder. The sintering temperature and pressure were set as follows. First, the temperature was increased from room temperature to 50 °C in 1 min, then to 500 °C at 45 °C/min, and held there for 10 min while applying a pressure of 6 MPa. Then, the following measurements were carried out to obtain the optical and radiation-induced luminescence characteristics.

## 2.2 Equipment and measurement conditions

The morphologies of the ACC ceramic surfaces were analyzed using a scanning electron microscope (JCM-6000Plus, JEOL). The diffuse transmission spectra of the ACC translucent ceramics were measured using a spectrophotometer (SolidSpec-3700, Shimadzu) across a spectral range from 200 to 800 nm with 1 nm intervals. The X-ray-induced scintillation spectrum was measured using our laboratory-made setup. We used an X-ray generator (XRB80N100/CB, Spellman) and a CCD-based detector (Shamrock 163 monochromator and DU-420-BU2 CCD, Andor). The PL excitation/emission spectra were obtained using a spectrofluorometer (FP-8600, JASCO) equipped with a Xe lamp as an excitation source.

To investigate the effects of X-ray irradiation on the optical properties of ACC translucent ceramics, the specimen was irradiated with different X-ray irradiation doses using an X-ray generator (XRB80P&N200X4550, Spellman) equipped with a W target. The X-ray irradiation dose was controlled by changing the irradiation time (6–60 s) and tube current (0.052–5.2 Ma). The X-ray tube was operated at a fixed voltage of 40 kV, and the mean energy was 15–20 keV. The values of dose refer to dose in the air at the entrance of the specimen, and the irradiation dose was calibrated using an air-filled ionization chamber (Model 30013, PTW).

## 3. Results and Discussion

Figure 1 shows photographs of the 0.03 and 1.0% Au-doped specimens under white LED light. The transmittance in the VIS region changed significantly depending on the concentration of Au doping. The back of the specimen can be clearly observed for the 0.03% Au-doped specimen, whereas it is barely observable for the 1.0% Au-doped specimen. It is considered that Au affects the optical properties of CsCl ceramics by changing the particle state and interacting with Au itself and light.

The effects of Au doping on the morphology and surface roughness of the specimens have been investigated by SEM. Figure 2 shows the SEM images of the 0.03% and 1.0% Au-doped specimens. It is observed that the surface morphologies of the specimens consist of several grains of micrometer size. Figure 3 shows the variation in particle size distribution with different concentrations of Au in the specimens. The distribution of particles represented by the histograms revealed that the average grain size increased when the Au concentration was increased. This result suggests that Au promotes grain growth during sintering. Generally, grain growth in the sintering process creates some voids, which increase the number of light scattering sources, and they can reduce transmittance in translucent ceramics. In addition, some of the doping ions (Au) are present as impurities intervening at the grain boundary and also decrease the translucency. Then, the transparency of the specimen doped with more AuCl was lower as shown in Fig. 1.

Figure 4 shows the diffuse transmission spectra of the specimen obtained before and after X-ray irradiations. Figure 4(a) shows that the transmittance in the UV-to-NIR region of the specimens was around 60% at most, and especially below 40% in the VIS region. The transmittance of the 1.0% Au-doped specimen in the VIS region was lower than that of the

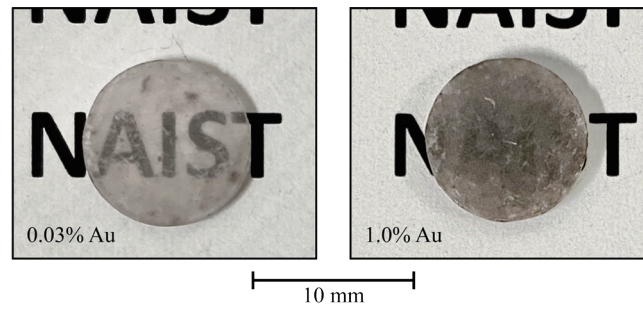


Fig. 1. Photographs of ACC translucent ceramics doped with 0.03 and 1.0% Au under white LED light.

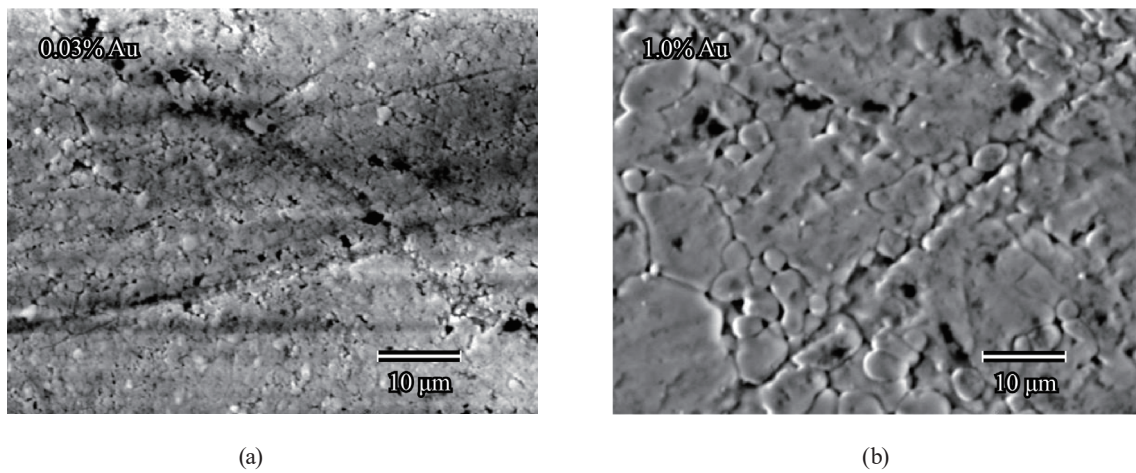


Fig. 2. SEM images of ACC translucent ceramics doped with (a) 0.03 and (b) 1.0% Au.

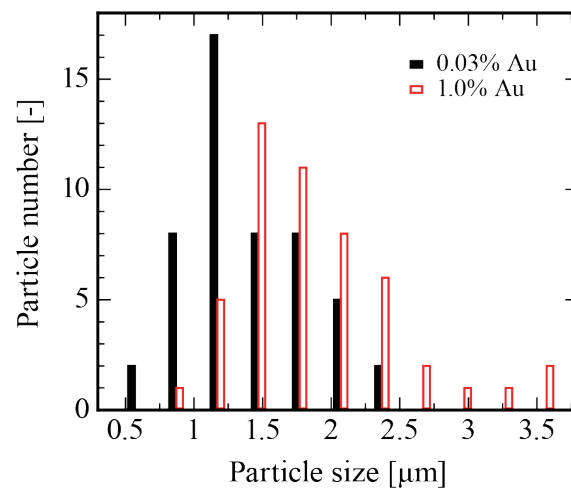


Fig. 3. (Color online) Particle size distribution of ACC translucent ceramics with different Au concentrations.

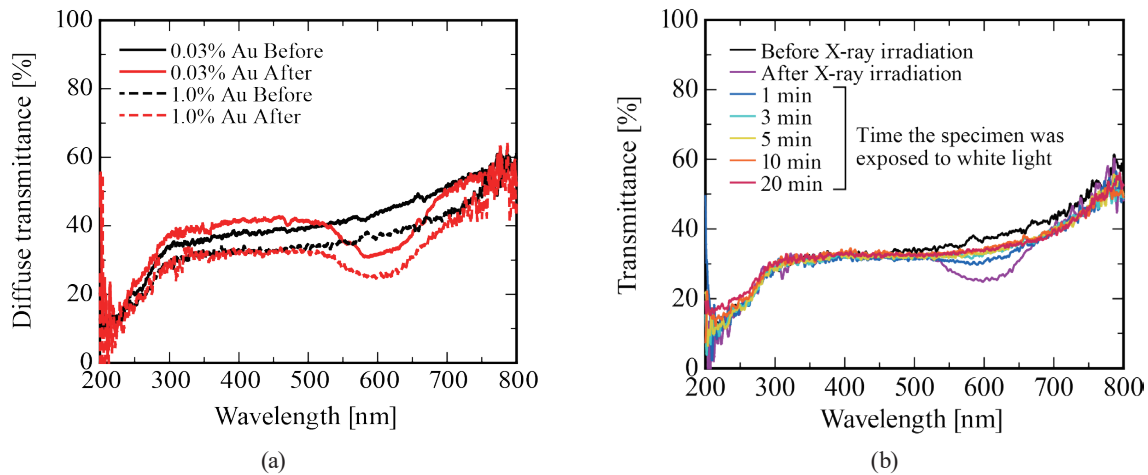


Fig. 4. (Color online) Diffuse transmission spectra of ACC translucent ceramics before and after X-ray irradiations. (a) Transmission spectra of 0.03% and 1.0% Au-doped specimens. (b) Transmission spectra of 1.0% Au-doped specimen before and after a certain period of time elapsed after X-ray irradiation.

0.03% counterpart, consistent with the appearance of the specimens shown in Fig. 1. This absorption can be attributed to defects generated by the doping of AuCl and/or to the precipitation of metallic Au.<sup>(50)</sup> After irradiating X-rays (~1 Gy) for the specimens, an absorption band at around 600 nm appeared, which is typical for alkali halides. The origin of this absorption band is the F-center where electrons entered into Cl defects.<sup>(31,51)</sup> Figure 4(b) shows the transmission spectra of the 1.0% Au-doped specimen obtained before and after a certain period of time elapsed after X-ray irradiation. The absorption band due to the F-center disappeared with time by exposing the specimen under white light. This phenomenon is called bleaching, and it is known that color centers such as the F-center in halides disappear upon photo or thermal stimulation;<sup>(52)</sup> the F-center in CsCl is also bleached by heat at about room temperature in addition to the photochemical bleaching.<sup>(47,48)</sup> The absorption band reverted to a spectrum almost equivalent to that before irradiation after 10 min of exposure to white light at room temperature, and no further spectral change was observed after more time. The decrease in transmittance from 500 to 700 nm in the spectrum after X-ray irradiation compared with that before X-ray irradiation is considered to be due to an absorption attributed to the SPR of AuNPs, which was generated by X-ray irradiation.<sup>(50,53,54)</sup>

In the 0.03% Au-doped specimen, the luminescence that can be related to Au could not be confirmed almost completely. Thus, only the 1.0% Au-doped specimen will be discussed in the following sections. Figure 5 shows the X-ray-induced scintillation spectrum of the specimen. Several characteristic emissions were observed in the spectra; in particular, the luminescence around ~400 nm was the most prominent. The strong luminescence at ~400 nm is attributed to the complex band of off-center self-trapped exciton (STE) and defects,<sup>(55,56)</sup> and the shoulder observed at ~350 nm is also due to extrinsic defects.<sup>(55,57)</sup> The other two weak emissions of ~245 and ~275 nm are attributed to Auger-free luminescence (AFL).<sup>(46,58)</sup> Moreover, a very weak luminescence was observed at around 500 and 600 nm. This luminescence can be attributed to the Au-related luminescence, since no luminescence was observed in CsCl under ~340 nm

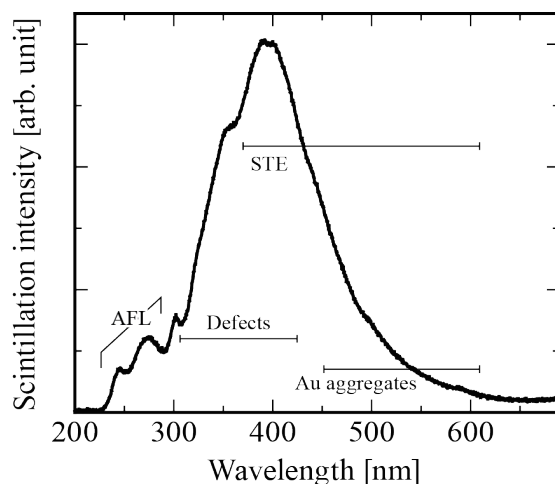


Fig. 5. X-ray-induced scintillation spectrum of ACC translucent ceramics.

excitation. According to previous reports, Au atoms in solids or liquids aggregate to form dimers, AuNCs, and AuNPs.<sup>(59–62)</sup> These Au aggregates emit light in a wide range of wavelengths from the VIS-to-NIR region, depending on the matrix material and aggregation state. Thus, the luminescence observed at 500–600 nm is reasonable for luminescence from Au aggregates. Considering the luminescent wavelength, the AuNP size is considered to be several tens of nanometers.<sup>(44)</sup>

Figure 6 shows the emission spectra obtained before and after the X-ray irradiation of the specimen under  $\sim 340$  nm excitation. The spectra were measured after X-ray irradiation and after the spectral intensity had stabilized (after more than a few tens of minutes). The irradiation dose to the specimen was 10 Gy. Only a broad luminescence at 600–1000 nm was observed in the spectrum before X-ray irradiation. On the other hand, after X-irradiation, part of the luminescence band that had been observed before irradiation disappeared, and new luminescence bands appeared around 420 and 520 nm. The disappearance of the luminescence at 600–700 nm can be attributed to the F-center in CsCl and the SPR of AuNPs, as shown in Fig. 4.

Figure 7(a) shows the change over time in the PL spectrum after X-ray irradiation. The luminescence intensity in the VIS region decreased monotonically with time, while that in the NIR region increased rapidly for about 10 s and then decreased monotonically. Here, we will focus on the luminescence in the NIR region, where the variation in response to radiation is significant. There are two possible factors for the behavior of luminescence in the NIR region: (i) RPL and (ii) excitation of AuNCs associated with the disappearance of F-centers. (i) In a previous report on the PL properties of Au in glass, the Au dimer in the complex is fragmented from the complex by UV light irradiation, resulting in a decrease in luminescence from the dimer of the complex ( $\sim 520$  nm) and an increase in the luminescence ( $\sim 720$  nm) of the newly generated pure Au dimer.<sup>(62)</sup> The behavior of PL in our specimen is very similar to the above, and it is highly plausible that Au dimers or equivalent aggregates in CsCl are involved in a similar mechanism. (ii) The bleaching of the absorption band attributed to the F-center can occur at the same time as the change in luminescence intensity. Thus, the electrons released from the F-center recombined with nearby holes, and the recombination energy excited the AuNCs, which

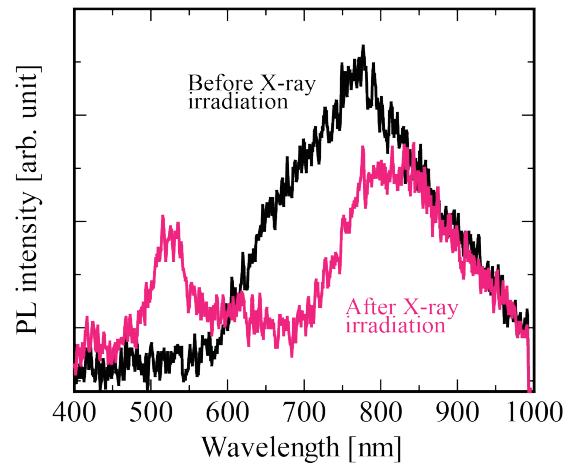


Fig. 6. (Color online) PL spectra obtained before and after X-ray irradiations of ACC translucent ceramics.

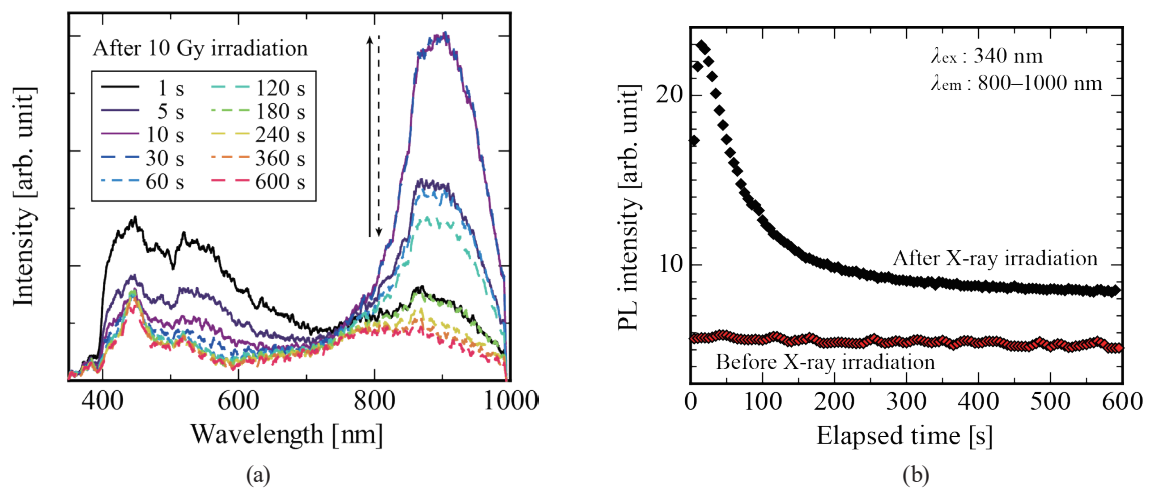


Fig. 7. (Color online) (a) PL spectra of ACC translucent ceramics under  $\sim 340$  nm excitation after a certain time interval from X-ray irradiation. (b) Variation with time of the integrated intensity of luminescence in the NIR region of 800–1000 nm before and after X-ray irradiation. The excitation wavelength was  $\sim 340$  nm.

seems to increase the luminescence intensity (a type of OSL). Regarding the decrease in the luminescence intensity, the decomposition of Au aggregates shortly after their formation is considered to be responsible, since Au aggregates are often unstable.<sup>(63–65)</sup>

Figure 7(b) shows the variation with time of the integrated intensity of luminescence in the NIR region of 800–1000 nm before and after X-ray irradiation. On the other hand, after X-ray irradiation, the luminescence intensity increased significantly within a few seconds after excitation and then decreased exponentially. The luminescence intensity had not completely returned to the initial state at 600 s, and the baseline had increased. This result supports hypothesis (i), as new luminescent centers are generated by X-ray irradiation.

Figure 8 shows the plot of time integration over 600 s for 800–1000 nm luminescence versus the irradiation dose of the specimen. The time integration of the luminescence intensity over 600

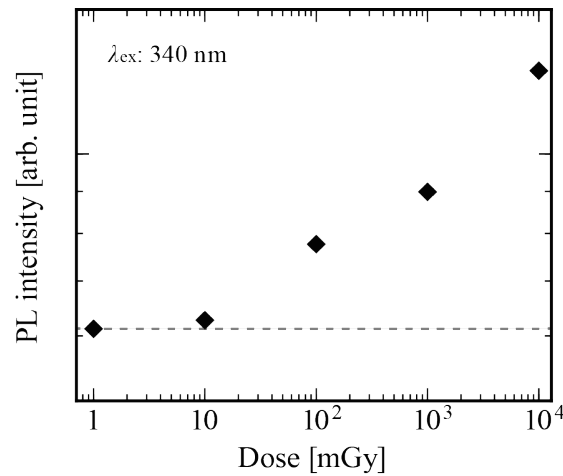


Fig. 8. Plot of time integration over 600 s for NIR luminescence in the 800–1000 nm range versus irradiation dose of ACC translucent ceramic specimen.

s increased monotonically in the region above several tens of mGy. These results suggested that the specimen can function as a dosimeter in the high dose range.

#### 4. Conclusions

The CsCl translucent ceramic containing Au particles was successfully prepared by SPS. The specimen showed luminescence attributed to Au aggregates under excitation at 340 nm, and the luminescence intensity was found to vary with X-ray irradiation dose and elapsed time after irradiation. Moreover, the time-integrated luminescence intensity was monotonically increased relative to the X-ray irradiation dose, suggesting that it has the potential to be applied to radiation detectors. On the other hand, the detailed origin and variation behavior of the observed luminescence have not yet been elucidated; therefore, detailed investigations are needed in the future.

#### Acknowledgments

This work was supported by Grants-in-Aid for Scientific Research A (17H01375 and 22H00309), B (21H03733 and 22H02939), Research Activity Start-up (22K20489 and 23K19188), and JSPS Fellows (20J23225). The Cooperative Research Project of the Research Center for Biomedical Engineering is also acknowledged.



## References

- 1 T. Kato, D. Nakauchi, N. Kawaguchi, and T. Yanagida: *Jpn. J. Appl. Phys.* **62** (2023) 010604. <https://doi.org/10.35848/1347-4065/ac94ff>
- 2 S. F. Mohd Ridzwan, N. Bhoo-Pathy, L. H. Wee, and M. Isahak: *Ann. Work Expo. Heal.* (2021) <https://doi.org/10.1093/annweh/wxab025>
- 3 H. Yasuda, K. Yajima, and T. Sato: *Radiat. Meas.* **134** (2020) 106309. <https://doi.org/10.1016/j.radmeas.2020.106309>
- 4 P. Lecoq: *Nucl. Instrum. Methods Phys. Res., Sect. A* **809** (2016) 130. <https://doi.org/10.1016/j.nima.2015.08.041>
- 5 P. Moskal, N. Zoń, T. Bednarski, P. Białas, E. Czerwiński, A. Gajos, D. Kamińska, Ł. Kapłon, A. Kochanowski, G. Korcyl, J. Kowal, P. Kowalski, T. Kozik, W. Krzemień, E. Kubicz, S. Niedźwiecki, M. Pałka, L. Raczyński, Z. Rudy, O. Rundel, P. Salabura, N. G. Sharma, M. Silarski, A. Słomski, J. Smyrski, A. Strzelecki, A. Wieczorek, W. Wiślicki, and M. Zieliński: *Nucl. Instrum. Methods Phys. Res., Sect. A* **775** (2015) 54. <https://doi.org/10.1016/j.nima.2014.12.005>
- 6 Q. Liu, Y. Cheng, Y. Yang, Y. Peng, H. Li, Y. Xiong, and T. Zhu: *Appl. Radiat. Isot.* **163** (2020) 109217. <https://doi.org/10.1016/j.apradiso.2020.109217>
- 7 L. E. Sinclair, D. S. Hanna, A. M. L. MacLeod, and P. R. B. Saull: *IEEE Trans. Nucl. Sci.* **56** (2009) 1262. <https://doi.org/10.1109/TNS.2009.2019271>
- 8 A. Khan, P. Q. Vuong, G. Rooh, H. J. Kim, and S. Kim: *J. Alloys Compd.* **827** (2020) 154366. <https://doi.org/10.1016/j.jallcom.2020.154366>
- 9 A. Bala, D. G. Jenkins, and S. Namadi: *Dutse J. Pure Appl. Sci.* **8** (2022) 80. <https://doi.org/10.4314/dujopas.v8i2a.9>
- 10 E. Caroli, J. B. Stephen, G. Di Cocco, L. Natalucci, and A. Spizzichino: *Space Sci. Rev.* **45** (1987) 349. <https://doi.org/10.1007/BF00171998>
- 11 T. Yanagida, T. Kato, D. Nakauchi, and N. Kawaguchi: *Jpn. J. Appl. Phys.* **62** (2023) 010508. <https://doi.org/10.35848/1347-4065/ac9026>
- 12 N. Kawaguchi, K. Watanabe, D. Shiratori, T. Kato, D. Nakauchi, and T. Yanagida: *Sens. Mater.* **35** (2023) 499. <https://doi.org/10.18494/SAM4136>
- 13 D. Shiratori, H. Fukushima, D. Nakauchi, T. Kato, N. Kawaguchi, and T. Yanagida: *Jpn. J. Appl. Phys.* **62** (2023) 010608. <https://doi.org/10.35848/1347-4065/ac90a4>
- 14 T. Kunikata, T. Kato, D. Shiratori, P. Kantuptim, D. Nakauchi, N. Kawaguchi, and T. Yanagida: *Sens. Mater.* **35** (2023) 491. <https://doi.org/10.18494/SAM4145>
- 15 I. Kawamura, H. Kawamoto, Y. Fujimoto, M. Koshimizu, G. Okada, G. Wakabayashi, M. Nogami, K. Hitomi, K. Watanabe, T. Yanagida, and K. Asai: *Jpn. J. Appl. Phys.* **60** (2021) 036002. <https://doi.org/10.35848/1347-4065/abdf7d>
- 16 A. R. Kadam, G. C. Mishra, and S. J. Dhoble: *J. Mol. Struct.* **1225** (2021) 129129. <https://doi.org/10.1016/j.molstruc.2020.129129>
- 17 Z. G. P. Uçar, Ü. H. Kaynar, T. Dogan, G. O. Souadi, M. Ayvacikli, A. Canimoglu, M. Topaksu, and N. Can: *Opt. Mater.* **104** (2020) 109852. <https://doi.org/10.1016/j.optmat.2020.109852>
- 18 M. Bakr, Z. G. Portakal-Uçar, M. Yüksel, Ü. H. Kaynar, M. Ayvacikli, S. Benourdja, A. Canimoglu, M. Topaksu, A. Hammoudeh, and N. Can: *J. Lumin.* **227** (2020) 117565. <https://doi.org/10.1016/j.jlumin.2020.117565>
- 19 T. Yanagida, T. Kato, Y. Takebuchi, D. Nakauchi, and N. Kawaguchi: *Radiat. Meas.* **132** (2020) 106250. <https://doi.org/10.1016/j.radmeas.2020.106250>
- 20 N. Kawaguchi, G. Okada, Y. Futami, D. Nakauchi, T. Kato, and T. Yanagida: *Sens. Mater.* **32** (2020) 1419. <https://doi.org/10.18494/SAM.2020.2752>
- 21 K. Shinsho, R. Oh, M. Tanaka, N. Sugioka, H. Tanaka, G. Wakabayashi, T. Takata, W. Chang, S. Matsumoto, G. Okada, S. Sugawara, E. Sasaki, K. Watanabe, Y. Koba, K. Nagasaka, S. Yoshihashi, A. Uritani, and T. Negishi: *Jpn. J. Appl. Phys.* **62** (2023) 010502. <https://doi.org/10.35848/1347-4065/ac971e>
- 22 K. Ichiba, Y. Takebuchi, H. Kimura, D. Shiratori, T. Kato, D. Nakauchi, N. Kawaguchi, and T. Yanagida: *Sens. Mater.* **34** (2022) 677. <https://doi.org/10.18494/SAM3680>
- 23 H. Fukushima, D. Shiratori, D. Nakauchi, T. Kato, N. Kawaguchi, and T. Yanagida: *Sens. Mater.* **34** (2022) 717. <https://doi.org/10.18494/SAM3691>
- 24 S. W. S. McKeever, S. Sholom, and J. R. Chandler: *Radiat. Prot. Dosim.* **192** (2020) 205. <https://doi.org/10.1093/rpd/ncaa208>
- 25 M. C. S. Nunes, L. S. Lima, E. M. Yoshimura, L. V. S. França, O. Baffa, L. G. Jacobsohn, A. L. M. C. Malthez, R. Kunzel, and N. M. Trindade: *J. Lumin.* **226** (2020) 117479. <https://doi.org/10.1016/j.jlumin.2020.117479>

- 26 C. C. Lu, F. N. Wang, H. H. Lin, C. H. Hsu, J. P. Lin, and L. H. Lai: Radiat. Phys. Chem. **172** (2020) 108792. <https://doi.org/10.1016/j.radphyschem.2020.108792>
- 27 H. Nanto and G. Okada: Jpn. J. Appl. Phys. **62** (2023) 010505. <https://doi.org/10.35848/1347-4065/ac9106>
- 28 T. Kato, H. Kimura, K. Okazaki, D. Nakauchi, N. Kawaguchi, and T. Yanagida: Sens. Mater. **35** (2023) 483. <https://doi.org/10.18494/SAM4137>
- 29 G. Ito, H. Kimura, D. Shiratori, D. Nakauchi, T. Kato, N. Kawaguchi, and T. Yanagida: Sens. Mater. **34** (2022) 685. <https://doi.org/10.18494/SAM3681>
- 30 M. Iwao, H. Takase, D. Shiratori, D. Nakauchi, T. Kato, N. Kawaguchi, and T. Yanagida: Radiat. Meas. **140** (2021) 106492. <https://doi.org/10.1016/j.radmeas.2020.106492>
- 31 H. Kimura, G. Okada, T. Kato, D. Nakauchi, N. Kawaguchi, and T. Yanagida: J. Lumin. **236** (2021) 118099. <https://doi.org/10.1016/j.jlumin.2021.118099>
- 32 T. Kato, D. Shiratori, M. Iwao, H. Takase, D. Nakauchi, N. Kawaguchi, and T. Yanagida: Sens. Mater. **33** (2021) 2163. <https://doi.org/10.18494/SAM.2021.3318>
- 33 D. Shiratori, T. Kato, D. Nakauchi, N. Kawaguchi, and T. Yanagida: Sens. Mater. **33** (2021) 2171. <https://doi.org/10.18494/SAM.2021.3317>
- 34 H. Kawamoto, M. Koshimizu, Y. Fujimoto, and K. Asai: Jpn. J. Appl. Phys. **62** (2023) 010501. <https://doi.org/10.35848/1347-4065/ac9cb0>
- 35 D. Shiratori, Y. Takebuchi, T. Kato, D. Nakauchi, N. Kawaguchi, and T. Yanagida: Sens. Mater. **34** (2022) 745. <https://doi.org/10.18494/SAM3695>
- 36 G. Okada, Y. Koguchi, T. Yanagida, S. Kasap, and H. Nanto: Jpn. J. Appl. Phys. **62** (2023) 010609. <https://doi.org/10.35848/1347-4065/ac9023>
- 37 T. Kurobori and S. Nakamura: Radiat. Meas. **47** (2012) 1009. <https://doi.org/10.1016/j.radmeas.2012.09.003>
- 38 K. Ichiba, G. Okada, Y. Takebuchi, T. Kato, D. Shiratori, D. Nakauchi, N. Kawaguchi, and T. Yanagida: J. Lumin. **257** (2023) 119698. <https://doi.org/10.1016/j.jlumin.2023.119698>
- 39 A. Nishikawa, D. Shiratori, P. Kantuptim, T. Kato, D. Nakauchi, N. Kawaguchi, and T. Yanagida: J. Mater. Sci. - Mater. Electron. **34** (2023) 1121. <https://doi.org/10.1007/s10854-023-10514-7>
- 40 P. Zijlstra, J. W. M. Chon, and M. Gu: Nature **459** (2009) 410. <https://doi.org/10.1038/nature08053>
- 41 L. Qin, X. He, L. Chen, and Y. Zhang: ACS Appl. Mater. Interfaces **7** (2015) 5965. <https://doi.org/10.1021/acsami.5b00269>
- 42 W. Hou and S. B. Cronin: Adv. Funct. Mater. **23** (2013) 1612. <https://doi.org/10.1002/adfm.201202148>
- 43 M. A. Garcia, J. de la Venta, P. Crespo, J. LLopis, S. Penadés, A. Fernández, and A. Hernando: Phys. Rev. B: Condens. Matter **72** (2005) 241403. <https://doi.org/10.1103/PhysRevB.72.241403>
- 44 J. Zheng, C. Zhou, M. Yu, and J. Liu: Nanoscale **4** (2012) 4073. <https://doi.org/10.1039/c2nr31192e>
- 45 H. Rabin and J. H. Schulman: Phys. Rev. **125** (1962) 1584. <https://doi.org/10.1103/PhysRev.125.1584>
- 46 M. Fukaya, Y. Kayanuma, and M. Itoh: J. Phys. Soc. Jpn. **71** (2002) 2557. <https://doi.org/10.1143/JPSJ.71.2557>
- 47 P. Avakian and A. Smakula: Phys. Rev. **120** (1960) 2007. <https://doi.org/10.1103/PhysRev.120.2007>
- 48 F. Hughes and J. G. Allard: Phys. Rev. **125** (1962) 173. <https://doi.org/10.1103/PhysRev.125.173>
- 49 H. Kimura, T. Kato, T. Fujiwara, M. Tanaka, D. Nakauchi, N. Kawaguchi, and T. Yanagida: Jpn. J. Appl. Phys. **62** (2023) 010504. <https://doi.org/10.35848/1347-4065/ac916c>
- 50 D. Shiratori, D. Nakauchi, T. Kato, N. Kawaguchi, and T. Yanagida: Jpn. J. Appl. Phys. **61** (2022) SB1015. <https://doi.org/10.35848/1347-4065/ac2ab5>
- 51 T. Ishii and M. Ueta: J. Phys. Soc. Jpn. **18** (1963) 1460. <https://doi.org/10.1143/JPSJ.18.1460>
- 52 T. A. FULTON and D. B. FITCHEN: Phys. Rev. **179** (1969) 846. <https://doi.org/10.1103/PhysRev.179.846>
- 53 N. Uehara and Y. Numanami: Sens. Actuators, B **247** (2017) 188. <https://doi.org/10.1016/j.snb.2017.03.004>
- 54 A. Doron, E. Katz, and I. Willner: Langmuir **11** (1995) 1313. <https://doi.org/10.1021/la00004a044>
- 55 M. Itoh, K. Tanimura, and N. Itoh: J. Phys. Soc. Jpn. **62** (1993) 2904. <https://doi.org/10.1143/JPSJ.62.2904>
- 56 S. Zazubovich, A. Voloshinovskii, and G. Stryganyuk: Phys. Status Solidi **233** (2002) 238. [https://doi.org/10.1002/1521-3951\(200209\)233:2<238::AID-PSSB238>3.0.CO;2-E](https://doi.org/10.1002/1521-3951(200209)233:2<238::AID-PSSB238>3.0.CO;2-E)
- 57 H. Kimura, T. Kato, D. Nakauchi, M. Koshimizu, N. Kawaguchi, and T. Yanagida: Sens. Mater. **31** (2019) 1265. <https://doi.org/10.18494/SAM.2019.2186>
- 58 P. Jaeglé, S. Sebban, A. Carillon, G. Jamelot, A. Klisnick, P. Zeitoun, B. Rus, M. Nantel, F. Albert, and D. Ros: J. Appl. Phys. **81** (1997) 2406. <https://doi.org/10.1063/1.364246>
- 59 A. Nisar, H. Hapuarachchi, L. Lermusiaux, J. H. Cole, and A. M. Funston: ACS Appl. Nano Mater. **5** (2022) 3213. <https://doi.org/10.1021/acsnm.1c03522>
- 60 A. S. Krishna Kumar and W.-L. Tseng: Anal. Methods **12** (2020) 1809. <https://doi.org/10.1039/D0AY00157K>
- 61 N. Gao, Y. Chen, L. Li, Z. Guan, T. Zhao, N. Zhou, P. Yuan, S. Q. Yao, and Q.-H. Xu: J. Phys. Chem. C **118** (2014) 13904. <https://doi.org/10.1021/jp502038v>

- 62 M. Eichelbaum, K. Rademann, A. Hoell, D. M. Tatchev, W. Weigel, R. Stöber, and G. Pacchioni: *Nanotechnology* **19** (2008) 135701. <https://doi.org/10.1088/0957-4484/19/13/135701>
- 63 L. Xu, H.-W. Liang, Y. Yang, and S.-H. Yu: *Chem. Rev.* **118** (2018) 3209. <https://doi.org/10.1021/acs.chemrev.7b00208>
- 64 J. F. Parker, C. A. Fields-Zinna, and R. W. Murray: *Acc. Chem. Res.* **43** (2010) 1289. <https://doi.org/10.1021/ar100048c>
- 65 M. Reich, S. Utsunomiya, S. E. Kesler, L. Wang, R. C. Ewing, and U. Becker: *Geology* **34** (2006) 1033. <https://doi.org/10.1130/G22829A.1>